

Characterization of a Novel Pyranopyridine Inhibitor of the AcrAB Efflux Pump of *Escherichia coli*

Timothy J. Opperman, Steven M. Kwasny, Hong-Suk Kim,
Son T. Nguyen, Chad Houseweart, Sanjay D'Souza, Graham
C. Walker, Norton P. Peet, Hiroshi Nikaido and Terry L.
Bowlin
Antimicrob. Agents Chemother. 2014, 58(2):722. DOI:
10.1128/AAC.01866-13.
Published Ahead of Print 18 November 2013.

Updated information and services can be found at:
<http://aac.asm.org/content/58/2/722>

SUPPLEMENTAL MATERIAL	<i>These include:</i> Supplemental material
REFERENCES	This article cites 51 articles, 23 of which can be accessed free at: http://aac.asm.org/content/58/2/722#ref-list-1
CONTENT ALERTS	Receive: RSS Feeds, eTOCs, free email alerts (when new articles cite this article), more»

Information about commercial reprint orders: <http://journals.asm.org/site/misc/reprints.xhtml>
To subscribe to to another ASM Journal go to: <http://journals.asm.org/site/subscriptions/>

Characterization of a Novel Pyranopyridine Inhibitor of the AcrAB Efflux Pump of *Escherichia coli*

Timothy J. Opperman,^a Steven M. Kwasny,^a Hong-Suk Kim,^b Son T. Nguyen,^a Chad Houseweart,^{a†} Sanjay D'Souza,^c Graham C. Walker,^c Norton P. Peet,^a Hiroshi Nikaido,^b Terry L. Bowlin^a

Microbiotix, Inc., Worcester, Massachusetts, USA^a; Department of Molecular and Cell Biology, University of California, Berkeley, California, USA^b; Department of Biology, Massachusetts Institute of Technology, Cambridge, Massachusetts, USA^c

Members of the resistance-nodulation-division (RND) family of efflux pumps, such as AcrAB-TolC of *Escherichia coli*, play major roles in multidrug resistance (MDR) in Gram-negative bacteria. A strategy for combating MDR is to develop efflux pump inhibitors (EPIs) for use in combination with an antibacterial agent. Here, we describe MBX2319, a novel pyranopyridine EPI with potent activity against RND efflux pumps of the *Enterobacteriaceae*. MBX2319 decreased the MICs of ciprofloxacin (CIP), levofloxacin, and piperacillin versus *E. coli* AB1157 by 2-, 4-, and 8-fold, respectively, but did not exhibit antibacterial activity alone and was not active against AcrAB-TolC-deficient strains. MBX2319 (3.13 μ M) in combination with 0.016 μ g/ml CIP (minimally bactericidal) decreased the viability (CFU/ml) of *E. coli* AB1157 by 10,000-fold after 4 h of exposure, in comparison with 0.016 μ g/ml CIP alone. In contrast, phenyl-arginine- β -naphthylamide (PA β N), a known EPI, did not increase the bactericidal activity of 0.016 μ g/ml CIP at concentrations as high as 100 μ M. MBX2319 increased intracellular accumulation of the fluorescent dye Hoechst 33342 in wild-type but not AcrAB-TolC-deficient strains and did not perturb the transmembrane proton gradient. MBX2319 was broadly active against *Enterobacteriaceae* species and *Pseudomonas aeruginosa*. MBX2319 is a potent EPI with possible utility as an adjunctive therapeutic agent for the treatment of infections caused by Gram-negative pathogens.

Multidrug resistance (MDR) in Gram-negative pathogens, including *Enterobacteriaceae*, *Pseudomonas aeruginosa*, *Acinetobacter* spp., and *Stenotrophomonas maltophilia*, poses a significant threat to the effective treatment of infections caused by these organisms (1–4). The MDR threat has been exacerbated by the recent decrease in commercial efforts to discover and develop new antibacterial agents. In addition, antibacterial agents that have been introduced recently into the clinic or are in development, such as daptomycin, gemifloxacin, telithromycin, and telavancin, are not active against Gram-negative pathogens. Recently FDA-approved agents with activity against Gram-negative bacteria include tigecycline and doripenem. While tigecycline is active against bacteria producing a tetracycline-specific pump *in vitro*, it is pumped out rapidly by the ubiquitous multidrug pumps, and its pharmacokinetic properties limit its use for treating urinary tract infections (UTIs) and bloodstream infections (5), as will the evolution of resistance during therapy (6). Clearly, novel strategies for effectively treating infections caused by MDR Gram-negative pathogens are urgently needed.

The MDR phenotype has been attributed to both acquired and intrinsic mechanisms of resistance. However, the resistance-nodulation-division (RND) efflux pumps of Gram-negative bacteria play a major role in MDR. Because of their broad substrate specificity, overexpression of these efflux pumps results in decreased susceptibility to a diverse array of antibacterial agents and biocides (7). The major efflux pump of *Escherichia coli* is a typical resistance-nodulation-division (RND) pump, which is a tripartite structure consisting of an integral membrane efflux transporter with broad substrate specificity (AcrB), an outer membrane channel (TolC), and a periplasmic protein adapter (AcrA). Antibiotics enter the periplasmic space through a porin or by diffusion through the lipid bilayer, where they interact with the substrate-binding pocket of AcrB. The AcrB transporter uses the proton motive force to extrude the compound into the TolC channel and

to the exterior (8). These RND family pumps not only produce intrinsic levels of resistance to antibacterial agents, including the fluoroquinolones (FQs) (e.g., ciprofloxacin [CIP] and levofloxacin [LVX]), β -lactams (e.g., piperacillin [PIP], meropenem, and aztreonam) (9), and β -lactamase inhibitors (e.g., clavulanate and sulbactam) (10, 11), but also produce an MDR phenotype when overproduced (12). In addition, elimination of RND pumps in *P. aeruginosa* by genetic deletion (13) or inhibition with a potent efflux pump inhibitor (EPI) (14) decreases the frequency of resistance to levofloxacin. In *E. coli*, a functional AcrAB-TolC is required for selection of mutations in the targets of FQs (*gyrA* and *gyrB*) that give rise to FQ resistance (15). Furthermore, RND pumps have been shown to play a role in the virulence of the enteric pathogen *Salmonella enterica* serovar Typhimurium (16), and EPIs that target RND pumps have been shown to inhibit biofilm formation in *E. coli* and *Klebsiella pneumoniae* (17). Therefore, EPIs could be used as adjunctive therapies with an FQ or β -lactam antibiotic to improve antibacterial potency at low antibiotic concentrations, to reduce the emergence of resistance, to inhibit biofilm formation, and to decrease the virulence of enteric pathogens.

Several potent efflux pump inhibitors have been described in

Received 26 August 2013 Returned for modification 21 September 2013

Accepted 9 November 2013

Published ahead of print 18 November 2013

Address correspondence to Timothy J. Opperman, topperman@microbiotix.com.
† Deceased.

Supplemental material for this article may be found at <http://dx.doi.org/10.1128/AAC.01866-13>.

Copyright © 2014, American Society for Microbiology. All Rights Reserved.
doi:10.1128/AAC.01866-13

TABLE 1 Bacterial strains used in this study

Organism	Strain	Genotype/description	Reference or source
<i>Escherichia coli</i>	AB1157	<i>thr-1 araC14 leuB6(Am) Δ(gpt-proA)62 lacY1 tsx-33 qsr'-0 glnV44(AS) galK2(Oc) λ⁻ rac-0 hisG4(Oc) rfbC1 mgl-51 rpoS396(Am) rpsL31(Str^r) kdgK51 xylA5 mtl-1 argE3(Oc) thi-1</i>	51
<i>Escherichia coli</i>	Δ <i>tolC</i> mutant	AB1157 Δ <i>tolC::kan</i>	This study
<i>Escherichia coli</i>	Δ <i>acrB</i> mutant	AB1157 Δ <i>acrB::kan</i>	This study
<i>Escherichia coli</i>	Δ <i>acrF</i> mutant	AB1157 Δ <i>acrF::kan</i>	This study
<i>Escherichia coli</i>	Δ <i>macB</i> mutant	AB1157 Δ <i>macB::kan</i>	This study
<i>Escherichia coli</i>	Δ <i>emrB</i> mutant	AB1157 Δ <i>emrB::kan</i>	This study
<i>Escherichia coli</i>	285	AB1157 CIP ^r , overexpresses efflux ^a	This study
<i>Escherichia coli</i>	287	AB1157 CIP ^r , overexpresses efflux ^a	This study
<i>Escherichia coli</i>	331	CIP ^r , UTI isolate	Baylor College of Medicine
<i>Escherichia coli</i>	ATCC 25922		ATCC ^b
<i>Escherichia coli</i>	HN1157	F' <i>araD139 Δ(argF-lac)U169 rpsL150 rel-I flb-5301 ptsF25 deoCI thi-J ΔlamB106 ΔompF80 zei06::Tn10 ompCI24 acrR::kan</i>	35
<i>Escherichia coli</i>	HN1159	HN1157 Δ <i>acrAB::spc</i>	35
<i>Escherichia coli</i>	NCM3722	<i>E. coli</i> K-12 prototroph	52
<i>Enterobacter cloacae</i>	ATCC 13047		ATCC
<i>Enterobacter aerogenes</i>	ATCC 13048		ATCC
<i>Klebsiella pneumoniae</i>	ATCC 700603		ATCC
<i>Klebsiella pneumoniae</i>	ATCC 13882		ATCC
<i>Shigella flexneri</i>	ATCC 12022		ATCC
<i>Salmonella enterica</i> (typhimurium)	ATCC 14028		ATCC
<i>Pseudomonas aeruginosa</i>	PAO1		53
<i>Pseudomonas aeruginosa</i>	ATCC 27853		ATCC
<i>Proteus mirabilis</i>	ATCC 25933		ATCC
<i>Proteus mirabilis</i>	BAA-856	UTI clinical isolate	ATCC

^a Isolated as a ciprofloxacin-resistant mutant during serial passage with subinhibitory levels of ciprofloxacin.

^b ATCC, American Type Culture Collection.

the literature (18); however, none has reached clinical development. A family of peptidomimetics, including phenyl-arginine-β-naphthylamide (PAβN) (MC-207 110), exhibiting potent inhibition of efflux pumps in *P. aeruginosa*, has been developed for use as adjunctive therapy (14, 19–23). Some of these inhibitors were validated using *in vivo* infection models (20, 21, 23); however, they were abandoned because of toxicity (24). In addition, a series of pyridopyrimidine EPIs specific for the MexAB efflux pump of *P. aeruginosa* advanced to the preclinical stage (12, 25–30). In this paper, we describe the discovery and *in vitro* characterization of MBX2319, a novel pyranopyridine inhibitor of the RND class AcrAB-TolC efflux pump in *E. coli* and other pathogens of the *Enterobacteriaceae*.

MATERIALS AND METHODS

Strains and reagents. The strains used in this study are listed in Table 1. The following strains were obtained from the Keio collection (31): JW0451 (Δ*acrB::kan*), JW5503 (Δ*tolC::kan*), JW3234 (Δ*acrF::kan*), JW2661 (Δ*emrB::kan*), and JW0863 (Δ*macB::kan*). The deletion mutations in each of these strains were transferred to AB1157 using P1 phage transduction (Table 1). The construction of the *E. coli* cell-based reporter strain (SOS-1) that was used for high-throughput screening will be published elsewhere. Ciprofloxacin was purchased from ICN Biomedicals (Aurora, OH). Triclosan (Irgasan) was a generous gift from Ciba Specialty Chemicals, Inc. (High Point, NC). Hoechst 33342 (H33342) was purchased from Molecular Probes (Eugene, OR). The following reagents were purchased from Sigma-Aldrich (St. Louis, MO): phenyl-arginine-β-naphthylamide (PAβN), cyanide-*m*-chlorophenyl hydrazine (CCCP), levofloxacin, norfloxacin, nalidixic acid, piperacillin, cloxacillin, oxacil-

lin, chloramphenicol, tetracycline, ethidium bromide, gentamicin, crystal violet, cephalixin, amoxicillin, rifampin, cefotaxime, carbenicillin, novobiocin, erythromycin, linezolid, acriflavine, chlorhexidine, benzalkonium chloride, and cetylpyridinium chloride. β-D-[methyl-³H]Thiogalactopyranoside ([³H]TMG) (1 mCi/ml, 7 Ci/mmol) was obtained from Moravet Biochemicals (Brea, CA). Luria broth (LB) (Miller) and agar were purchased as prepared dehydrated media from Becton Dickinson (Franklin Lakes, NJ). The compound libraries used in high-throughput screens were purchased from ChemBridge (San Diego, CA), ChemDiv (San Diego, CA), and TimTec (Newark, DE).

Chemistry. The synthesis of MBX2319 is described in the supplemental material.

Antibacterial activity assays. The MICs of antibacterial agents and biocides were determined using the broth microdilution method, essentially as described in CLSI protocol M7-A7 (32) with the following exceptions. LB was used instead of Mueller-Hinton broth. Serial 2-fold dilutions of test compounds were made in dimethyl sulfoxide (DMSO) at concentrations 50-fold higher than the final concentration; the diluted compounds were added to the assay plates, and 100 μl of the bacterial culture was added to each well. The final concentration of DMSO in each assay was 2%. Where indicated, MIC assays were performed in the presence of an efflux pump inhibitor (EPI) at a final concentration of 25 μM. MIC assays were performed in triplicate, and the geometric mean was calculated. Checkerboard MIC assays using an EPI and an antibacterial agent were performed essentially as described previously (33), with the same modifications as used for the MIC assays described above.

Time-kill assays. Killing curve assays were performed essentially as described previously (33). Exponential bacterial cultures grown in LB were diluted to a cell density of ~1 × 10⁷ cells/ml in LB, followed by addition of CIP and/or an EPI. Viability was monitored over 2 to 4 h by

making serial dilutions in saline solution and spotting 5 μ l of each dilution onto the surface of an LB agar plate in triplicate. Colonies were counted after incubation of the plates at 37°C for 16 to 18 h, CFU/ml values were calculated, and the average and standard deviation for the three replicates were determined. For treatments that decreased CFU/ml values below the limit of detection for the spot plating method, the 100- μ l samples were diluted into 5 ml LB top agar, poured onto LB agar plates, and incubated at 37°C for 18 h. To calculate the fraction of the control for each sample, the average CFU/ml values for treated samples were divided by values for the same sample at 0 h (time 0). Each experiment was repeated at least three times, and a representative experiment is shown.

H33342 accumulation assay. The H33342 accumulation assay was used to evaluate the effect of EPIs on the activity of the AcrAB-TolC efflux pump in several bacterial species, essentially as described previously (34). Briefly, bacterial cultures were grown overnight in LB (Miller) with aeration at 37°C and were used to inoculate fresh cultures (1:100 dilution), which were grown in LB (Miller) with aeration until an optical density at 600 nm (OD_{600}) of 0.4 to 0.6 was reached. Bacterial cells were harvested by centrifugation, and the cell pellet was washed with a volume of phosphate-buffered saline (PBS) containing 1 mM $MgSO_4$ and 20 mM glucose (PBSM+G) equivalent to the original volume of the culture. After centrifugation, the cell pellets were resuspended in PBSM+G, and the OD_{600} of each suspension was adjusted to 0.2. Aliquots of 190 μ l were transferred to the wells of a 96-well assay plate (flat-bottom black plate, no. 3515; Costar, Corning, NY). Various concentrations of test compounds dissolved in DMSO or an equivalent volume of solvent alone were added to a total of 8 assay wells (one column of wells) for each condition tested. The final concentration of DMSO in all assays was 2%. The assay plates were incubated at 37°C for 15 min, and 10 μ l of a solution of 50 μ M H33342 in PBSM+G was added to each assay well, resulting in a final dye concentration of 2.5 μ M. The fluorescence (excitation and emission filters of 355 and 460 nm, respectively) of each well was measured at 37°C every 5 min for 30 min, using a Victor² V 1420 Multilabel HTS counter (PerkinElmer, Waltham, MA). The average values and standard deviations for the eight replicates for each condition were calculated using Microsoft Excel. Each experiment was repeated at least three times, and a representative experiment is shown.

Kinetics of nitrocefin efflux by AcrAB-TolC in *E. coli*. The effects of EPIs on the kinetic parameters of AcrAB-TolC in *E. coli* were estimated as described previously (35). Briefly, HN1157 was grown in modified LB broth, diluted 100-fold in fresh medium, and incubated at 30°C with shaking until the OD_{600} reached 0.65. The cells were harvested, washed twice (50 mM potassium phosphate buffer [pH 7.0], 5 mM $MgCl_2$), and resuspended in the same buffer at an OD_{600} of 0.8 (corresponding to 0.24 mg dry weight/ml). Nitrocefin was added at the desired final concentration, and the mixture was incubated at 25°C while the OD_{486} was measured over 30 min. The nitrocefin concentration in the periplasm (C_p) was calculated from the rate of hydrolysis (V_h) by the periplasmic β -lactamase and the kinetic constants of the β -lactamase, as described previously (35). The kinetic constants were derived by curve fitting of the velocity of AcrB (V_p) versus C_p values using GraphPad Prism version 5.04 (GraphPad), with the Michaelis-Menten equation. Each assay was repeated at least three times, and representative data are presented.

Uptake of [³H]TMG by the LacY permease. To estimate the effects of EPIs on the proton motive force in *E. coli* HN1157, the accumulation of [³H]TMG by the LacY permease was measured essentially as described previously (36). Briefly, a culture of NCM3722 cells (K-12 wild type [WT]) was grown at 37°C, with shaking, in LB containing 1 mM isopropyl β -D-1-thiogalactopyranoside (IPTG), was harvested at an OD_{600} of \sim 0.8, and was washed two times with 50 mM KH_2PO_4 buffer (pH 7.0), 5 mM $MgCl_2$ (PB). The cells were resuspended in PB, and the OD_{600} was adjusted to 0.8. The cell suspension was used immediately, without the further addition of an energy source. To 1 ml of cell suspension, 5 μ l of test compound solution (final concentrations of 0.2, 2, and 20 μ M), 20 mM CCCP (final concentration of 100 μ M; negative control), or DMSO (pos-

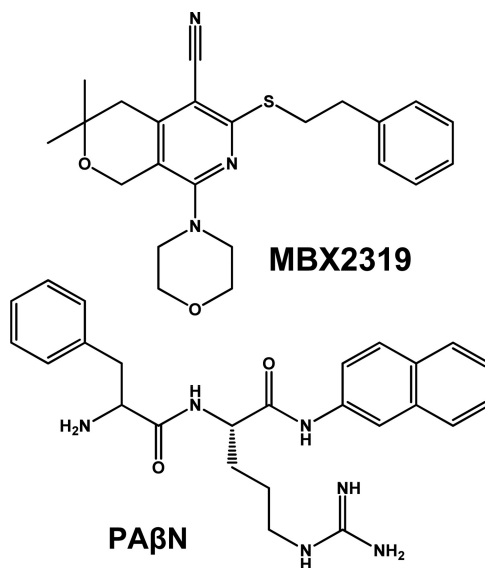


FIG 1 Structures of the efflux pump inhibitors MBX2319 and PA β N.

itive control) was added and preincubated for 10 min at room temperature. Then, an aliquot of 250 μ l of cells was removed and added to 5 μ l of a 5 mM [³H]TMG solution (final concentration, 0.1 mM; 10 μ Ci/ μ mol). After further incubation for 10 min, aliquots (200 μ l) were removed and filtered with a 0.45- μ m HA filter (diameter, 25 mm; Millipore, Billerica, MA). The filters were washed two times with 5 ml of PBB and counted with 5 ml of EcoLume scintillation cocktail (ICN Biomedicals, Costa Mesa, CA) in a Delta 300 liquid scintillation counting system (model 6891; TM Analytic, Elk Grove Village, IL).

Outer membrane integrity assay. HN1159 cells were grown in modified LB broth with 5 mM $MgSO_4$, diluted 500-fold in LB, and incubated at 30°C, with shaking, until the OD_{600} reached 0.65. The cells were harvested, washed twice (50 mM potassium phosphate buffer [pH 7.0]), and resuspended in the same buffer at an OD_{600} of 0.65. The cell suspension was transferred to the wells of an assay plate containing compound or solvent, nitrocefin was added at a final concentration of 75 μ M, OD_{486} was measured over 20 min, and the velocity of hydrolysis (V_h) was calculated.

Cytotoxicity assay. The cytotoxicity of MBX2319 against a mammalian cell line (HeLa, ATCC CCL-2) was determined as described previously (37). The compound concentration that inhibited the conversion of the vital stain MTT [3-(4,5-dimethyl-2-thiazolyl)-2,5-diphenyl-2H-tetrazolium bromide] to formazan by 50% (CC_{50}), in comparison with an untreated control, was determined using the 4-parameter curve-fitting program contained in GraphPad Prism version 5.04. The assay was performed in triplicate in at least two separate experiments.

RESULTS

Identification of MBX2319. To identify compounds that act synergistically with ciprofloxacin (CIP), we developed a cell-based reporter assay that reports on both SOS-1 cell induction and viability. Using the cell-based reporter assay, we screened 183,400 compounds and identified 1,782 primary hits, which were evaluated in a panel of secondary assays for prioritization based on potency and specificity. The details of the screening and secondary assays will be published elsewhere. Based on the results of these analyses, MBX2319 (Fig. 1) was chosen for further study.

MBX2319 potentiates the antibacterial activity of fluoroquinolone and β -lactam antibiotics against *E. coli*. We utilized a checkerboard assay to determine whether MBX2319 potentiates

TABLE 2 MBX2319 potentiates the antibacterial activity of fluoroquinolone and β -lactam antibiotics against *E. coli* strains that are efflux proficient and efflux overexpressers but not against Δ *acrB* or Δ *tolC* mutants

Strain	MBX2319 MIC (μ M)	Drug ^a	MIC (μ g/ml) for MBX2319 and a drug concentration of:							MIC ratio for:		
			0 μ M	1.56 μ M	3.13 μ M	6.25 μ M	12.5 μ M	25 μ M	50 μ M	MBX2319 ^b	Mutant ^c	
AB1157 (WT)	≥ 100	CIP	0.016	0.008	0.008	0.008	0.008	0.008	0.008	0.008	2	1
		LVX	0.063	0.031	0.016	0.016	0.016	0.016	0.016	0.016	4	1
		PIP	4	2	1	1	0.5	0.5	0.5	0.5	8	1
Δ <i>tolC</i> mutant	≥ 100	CIP	0.004	0.004	0.004	0.004	0.004	0.004	0.004	0.004	1	4
		LVX	0.016	0.016	0.016	0.008	0.008	0.008	0.008	0.008	2	4
		PIP	0.125	0.125	0.125	0.125	0.125	0.125	0.125	0.125	1	32
Δ <i>acrB</i> mutant	≥ 100	CIP	0.004	0.004	0.004	0.004	0.004	0.004	0.004	0.004	1	4
		LVX	0.016	0.016	0.016	0.016	0.016	0.016	0.016	0.016	1	4
		PIP	0.250	0.125	0.125	0.125	0.125	0.125	0.125	0.125	2	16
Δ <i>acrF</i> mutant	≥ 100	CIP	0.016	0.008	0.008	0.008	0.008	0.008	0.008	0.008	2	1
		LVX	0.063	0.031	0.031	0.016	0.016	0.016	0.016	0.016	4	1
		PIP	4	2	1	0.5	0.5	0.5	0.5	0.5	8	1
285 (EOE) ^d	≥ 100	CIP	1	0.25	0.125	0.125	0.125	0.125	0.125	0.125	8	0.016
		LVX	2	0.5	0.25	0.25	0.25	0.25	0.25	0.25	8	0.031
		PIP	8	4	2	2	2	2	2	2	4	0.5
285 Δ <i>tolC</i>	≥ 100	CTX	0.25	0.125	0.063	0.063	0.063	0.063	0.031	0.031	8	0.25
		CIP	0.063	0.063	0.063	0.063	0.063	0.063	0.063	0.063	1	0.25
		LVX	0.063	0.063	0.063	0.063	0.063	0.063	0.063	0.063	1	1
287 (EOE)	≥ 100	PIP	0.25	0.25	0.25	0.25	0.25	0.25	0.25	0.25	1	16
		CTX	0.031	0.031	0.031	0.031	0.031	0.031	0.031	0.031	1	2
		CIP	1	0.5	0.25	0.25	0.25	0.25	0.25	0.25	4	0.016
287 Δ <i>tolC</i>	≥ 100	LVX	2	0.5	0.5	0.5	0.5	0.25	0.25	0.25	8	0.031
		PIP	16	8	4	4	2	2	2	2	8	0.25
		CTX	0.25	0.125	0.125	0.063	0.063	0.063	0.063	0.063	4	0.25
287 Δ <i>tolC</i>	≥ 100	CIP	0.125	0.125	0.125	0.125	0.125	0.125	0.125	0.125	1	0.125
		LVX	0.125	0.125	0.125	0.125	0.125	0.125	0.125	0.125	1	0.5
		PIP	0.25	0.25	0.25	0.25	0.25	0.25	0.25	0.25	1	16
287 Δ <i>tolC</i>	≥ 100	CTX	0.015	0.015	0.015	0.015	0.015	0.015	0.015	0.015	1	4

^a CIP, ciprofloxacin; LVX, levofloxacin; PIP, piperacillin; CTX, cefotaxime.

^b Highest ratio of MIC with no compound to MIC with MBX2319.

^c MIC for WT/MIC for mutant in the absence of an EPI.

^d EOE, efflux overexpresser.

the activity of two fluoroquinolones, ciprofloxacin (CIP) and levofloxacin (LVX), and a β -lactam, piperacillin (PIP), against *E. coli* AB1157. The results, shown in Table 2, demonstrate that MBX2319 at 12.5 μ M decreased the MICs of CIP, LVX, and PIP by 2-, 4-, and 8-fold, respectively. MBX2319 alone did not exhibit antibacterial activity (MIC, ≥ 100 μ M). In addition, MBX2319 increased the bactericidal activity of 0.016 μ g/ml CIP (1 \times MIC), which is minimally bactericidal against *E. coli* AB1157, in a dose-dependent manner (Fig. 2A). The highest concentration of MBX2319 (3.13 μ M) decreased viability (CFU/ml) by 10,000-fold after 4 h of exposure, in comparison with CIP alone at 1 \times MIC. In contrast, MBX2319 alone at concentrations up to 50 μ M did not affect growth. For comparison, we measured the effects of various concentrations of phenyl-arginine- β -naphthylamide (PA β N), a known EPI (14), in combination with 0.016 μ g/ml CIP in the time-kill assay. The results of the assay are shown in Fig. 2B and demonstrate that PA β N at concentrations as high as 100 μ M did not increase the bactericidal activity of 0.016 μ g/ml CIP. This finding is consistent with a previous report that showed that PA β N at a concentration of 25 mg/ml (48 μ M) had a limited effect on the antibacterial activity of fluoroquinolones against *Enterobacteriaceae* (38).

MBX2319 is an efflux pump inhibitor. To verify that the mechanism by which MBX2319 potentiates the antibacterial ac-

tivity of fluoroquinolones and β -lactams is through inhibition of efflux, we determined whether MBX2319 potentiated the antibacterial activity of CIP, LVX, and PIP against a panel of efflux-defective mutants of *E. coli* AB1157. We reasoned that the antibiotic sensitivity of mutants lacking the target of MBX2319 would not be affected by the compound. The results of a checkerboard assay, shown in Table 2, demonstrate that the MICs for the Δ *tolC* and Δ *acrB* mutants were not affected by MBX2319, whereas mutants defective in other pumps that interact with TolC, such as AcrF (Table 2), MacB, and EmrB (data not shown), exhibited MIC shifts similar to those of the WT (AB1157). Similarly, MBX2319 potentiated the bactericidal activity of CIP against the Δ *acrF* strain but not against the Δ *tolC* and Δ *acrB* strains (Fig. 2C). Finally, MBX2319 potentiated the antibacterial activity of CIP, LVX, and PIP by 4- to 8-fold against *E. coli* strains 285 and 287 (Table 2), which are CIP-resistant mutants of *E. coli* AB1157 that were selected during serial passage with subinhibitory concentrations of CIP and exhibit increased efflux activity (see the supplemental material). Significantly, MBX2319 reduced the MICs against *E. coli* strains 285 and 287 to levels comparable to those obtained against isogenic efflux-defective mutants (Δ *tolC*). These findings indicate that the AcrAB-TolC efflux pump, which is the major efflux pump in *E. coli* (39), is a target of MBX2319. However, because deletion mutations of *acrF*, *acrD*, *macB*, and *emrB* do not

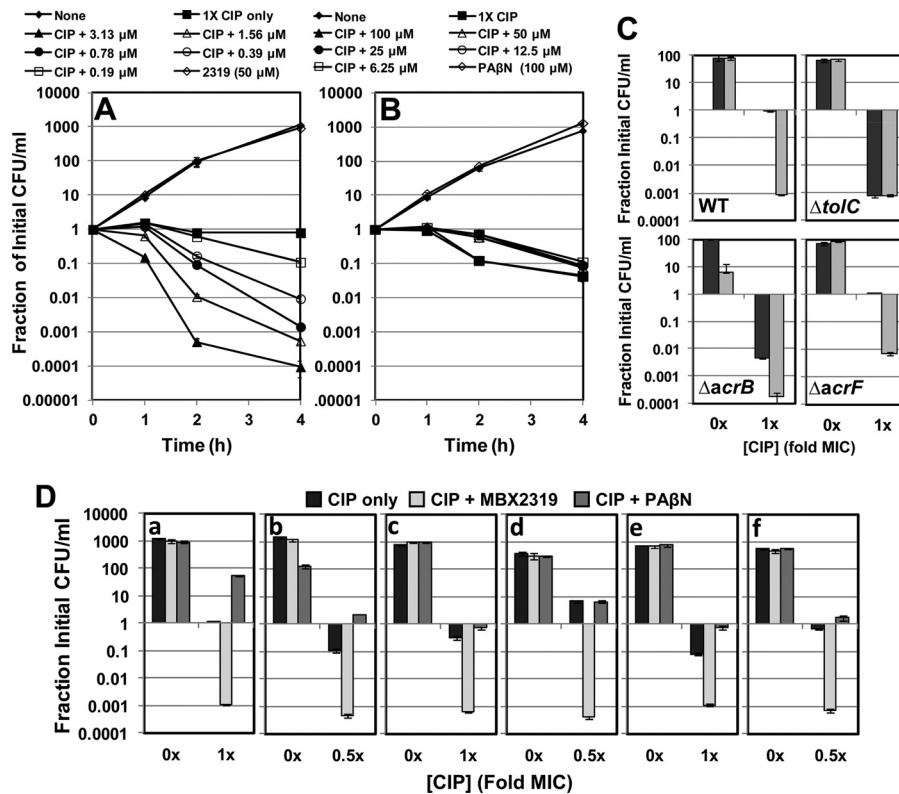


FIG 2 Effects of the efflux pump inhibitors MBX2319 and PAβN on the bactericidal activity of ciprofloxacin (CIP) in time-kill assays. (A) Bactericidal activity of varying concentrations of MBX2319 (0.19 to 3.13 μM) combined with a bacteriostatic concentration of CIP (1× MIC, 0.01 μg/ml) against *E. coli* AB1157. (B) Bactericidal activity of varying concentrations of PAβN (6.25 to 100 μM) combined with a minimally bactericidal concentration of CIP (1× MIC, 0.01 μg/ml) against *E. coli* AB1157. (C) Bactericidal activity of 25 μM MBX2319 combined with a minimally bactericidal concentration of CIP against *E. coli* AB1157 and isogenic efflux-defective mutants after 2 h of exposure. Black bars, CIP alone (1× MIC, 0.01 μg/ml); gray bars, CIP plus 25 μM MBX2319. (D) Bactericidal activity of 25 μM MBX2319 combined with a minimally bactericidal concentration of CIP against *E. coli* AB1157 (a), *E. coli* ATCC 25922 (b), *K. pneumoniae* ATCC 700603 (c), *S. flexneri* ATCC 12022 (d), *S. enterica* ATCC 14028 (e), and *E. aerogenes* ATCC 13048 (f).

affect susceptibility to the antibiotics used in this study, our results do not rule out the possibility that MBX2319 also inhibits the efflux pumps encoded by those genes.

To confirm that MBX2319 directly inhibits efflux, we used an assay that measures accumulation of the fluorescent DNA-binding dye Hoechst 33342 (H33342), which is a substrate of the AcrAB-TolC pump, in *E. coli* AB1157 (34). This assay has been used to estimate efflux activity in *E. coli* and *S. enterica* (34). When H33342 enters the cell, it binds to the DNA minor groove, becomes fluorescent, and can be detected using a fluorescent plate reader (with excitation at 355 nm and emission at 460 nm). Efflux-competent cells extrude H33342 and accumulate the dye at a relatively low rate, resulting in low levels of fluorescence. Conversely, efflux-defective cells accumulate H33342 at a higher rate, resulting in increased levels of fluorescence. The results of the H33342 accumulation assay are shown in Fig. 3A and B. The ΔacrB strain was used as a positive control, indicating the maximum levels of H33342 accumulation possible. MBX2319 (Fig. 3A) and PAβN (Fig. 3B) increased accumulation of H33342, in comparison with the untreated control, in a dose-dependent manner, although not linearly for MBX2319 at higher concentrations (25 to 50 μM) that approached the aqueous solubility limit. MBX2319 did not increase accumulation of H33342 in the ΔacrB and ΔtolC strains (Fig. 3C), which is consistent with the hypothesis that AcrAB-TolC is the target. At a concentration of 25 μM, MBX2319

and PAβN increased H33342 accumulation to levels that were about 45% and 52%, respectively, of those of the ΔacrB strain. MBX2319 was more effective in this assay at lower concentrations (3.1 to 12.5 μM) than was PAβN. Both compounds increased H33342 accumulation in the hyperflux strains 285 and 287 (Fig. 3D).

Finally, we measured the effects of MBX2319 and PAβN on the real-time efflux of nitrocefin by the AcrB efflux pump in intact cells (35). This assay measures the rate of nitrocefin hydrolysis by the AmpC β-lactamase as a function of the external nitrocefin concentration, to estimate the periplasmic concentration (C_p) of nitrocefin, which can be used to estimate the K_m and the maximum rate of metabolism (V_{max}) for the AcrAB-TolC efflux pump. The assay was repeated 12 times with and without 0.2 μM MBX2319, and clear inhibition of efflux was seen in all cases except one. Typical data are shown in Fig. 4A, in which curve-fitting suggests that most of the inhibition occurred through a large (4.4-fold) increase in the K_m . Although the curve-fitting also suggested that there was a marginal (2-fold) increase in the V_{max} , this is of uncertain significance, because the fitting had to be done in a quasi-linear portion of the plot. In most other assays, MBX2319 caused little change in the V_{max} (not shown). These data are consistent with the notion that MBX2319 competes with nitrocefin for the binding site or decreases access to the binding site. Higher concentrations of MBX2319 (1 to 10 μM) completely inhibited nitro-

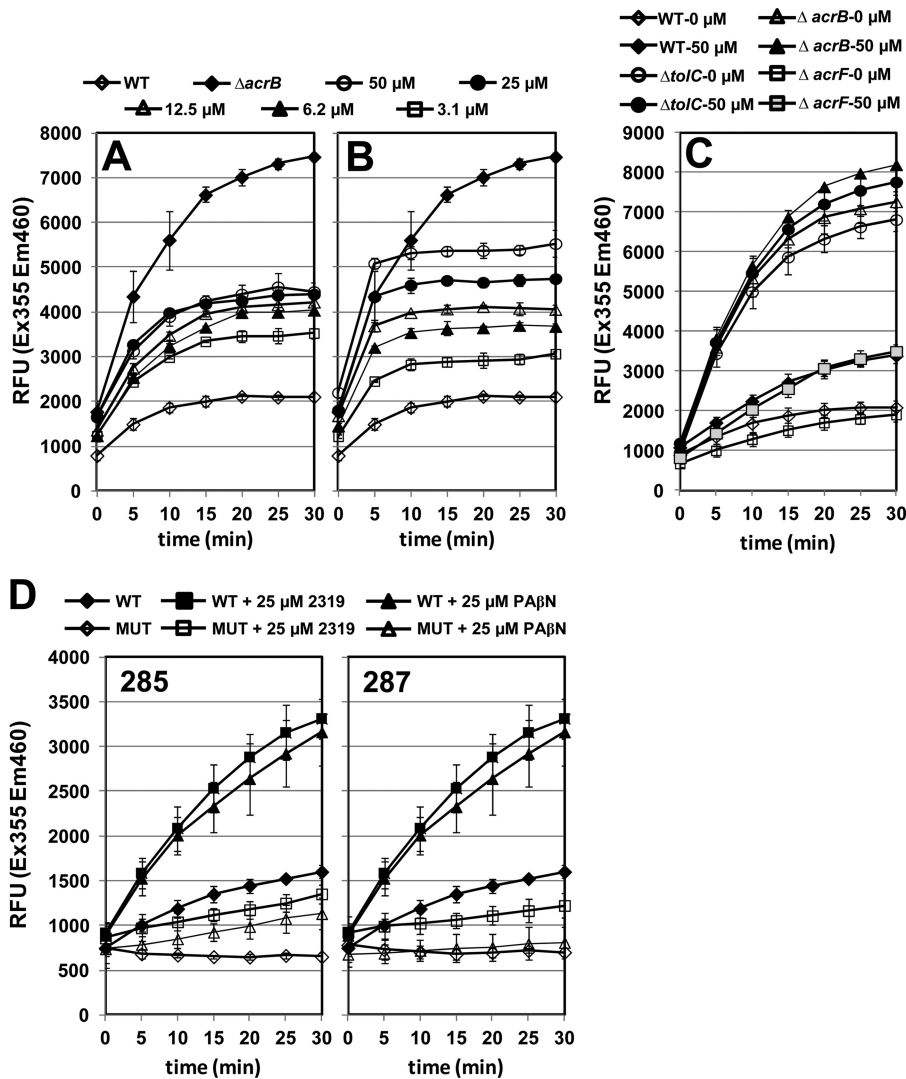


FIG 3 (A and B) Effects of MBX2319 (A) and PA β N (B) on accumulation of the fluorescent DNA-binding dye H33342, an AcrAB efflux pump substrate, in *E. coli* AB1157. (C) Effects of MBX2319 on H33342 accumulation in *E. coli* AB1157 and isogenic efflux-defective mutants. (D) Effects of MBX2319 on H33342 accumulation in *E. coli* AB1157 and isogenic mutants (MUT) 285 and 287, which exhibit reduced susceptibility to ciprofloxacin due to overexpression of efflux pumps. RFU, relative fluorescence units.

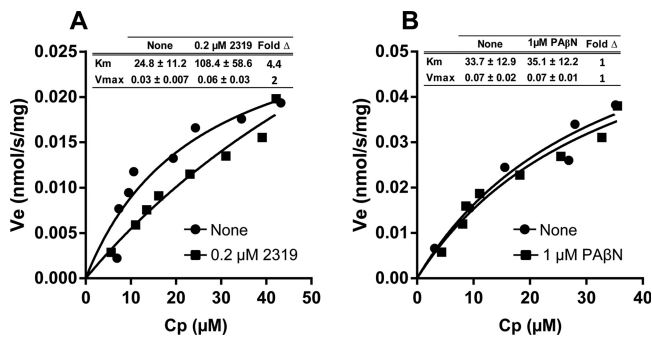


FIG 4 Effects of MBX2319 and PA β N on the kinetic parameters (K_m and V_{max}) of the AcrAB-TolC efflux pump in intact *E. coli* HN1157 cells using the nitrocefin efflux assay. (A) *E. coli* HN1157 cells treated with 0.2 μ M MBX2319 (2319). (B) *E. coli* HN1157 cells treated with 1 μ M PA β N.

cefin efflux and prevented kinetic analyses. In contrast, PA β N at concentrations ranging from 0.2 to 10 μ M had no effect on the efflux of nitrocefin, suggesting that this compound does not directly affect AcrB function in this range of concentrations. A representative result for an assay performed using 1 μ M PA β N is shown in Fig. 4B.

MBX2319 potentiates multiple antibiotics and biocides. Efflux pump inhibitors are known to increase the antibacterial activity of a diverse group of antibiotics and biocides. To test this prediction, we measured the ability of MBX2319 to increase the susceptibility of *E. coli* AB1157 to a broad spectrum of antibiotics and biocides. The data, shown in Table 3, demonstrate that MBX2319 increased susceptibility to several known AcrAB-TolC substrates, including CIP, LVX, nalidixic acid, PIP, oxacillin, and chloramphenicol, but not to gentamicin and carbenicillin, which are not substrates (40). In general, the MIC shifts produced by MBX2319 were smaller than those of the Δ acrB and Δ tolC strains but were similar to those produced by PA β N for fluoroquinolone

TABLE 3 MBX2319 potentiation of the antibacterial activity of diverse antibacterial agents and biocides

Compound ^a	MIC ($\mu\text{g/ml}$) for ^b :					MIC ratio for:			
	WT with:			ΔacrB mutant, no EPI	ΔtolC mutant, no EPI	MIC ratio for:			
	No EPI	MBX2319	PA β N			MBX2319 ^c	PA β N ^d	ΔacrB mutant ^e	ΔtolC mutant ^f
CIP	0.016	0.008	0.031	0.008	0.004	2	0.5	2	4
LVX	0.063	0.016	0.031	0.016	0.016	4	2	4	4
Norfloxacin	0.063	0.031	0.125	0.031	0.031	2	0.5	2	2
Nalidixic acid	16	4	2	2	1	4	8	8	16
PIP	4	0.5	8	0.25	0.25	8	0.5	16	16
Cloxacillin	512	64	256	4	1	8	2	128	512
Oxacillin	512	64	128	4	1	8	4	128	512
Carbenicillin	4	8	16	2	1	0.5	0.25	2	4
Chloramphenicol	8	2	2	2	1	4	4	4	8
Tetracycline	2	1	2	0.5	0.5	2	1	4	4
Gentamicin	8	8	4	8	4	1	2	1	2
Rifampin	16	8	4	8	8	2	4	2	2
Novobiocin	128	128	128	16	2	1	1	8	64
Erythromycin	128	16	4	2	2	8	32	64	64
Linezolid	240	60	120	15	15	4	2	16	16
EtBr	256	256	256	32	8	1	1	8	32
CV	32	8	8	1	1	4	4	32	32
IRG	0.5	0.25	0.25	0.125	0.016	2	2	4	32
Acriflavine	32	32	32	4	4	1	1	8	8
Chlorhexidine	1	1	1	1	1	1	1	1	1
BAC	32	16	8	2	2	2	4	16	16
CPC	4	4	2	2	2	1	2	2	2

^a CIP, ciprofloxacin; LVX, levofloxacin; PIP, piperacillin; EtBr, ethidium bromide; CV, crystal violet; IRG, Irgasan (triclosan); BAC, benzalkonium chloride; CPC, cetylpyridinium chloride.

^b Geometric means of MICs from at least three replicate experiments are presented. The final concentration of the EPIs MBX2319 and PA β N was 25 μM .

^c MIC with no compound/MIC with 25 μM MBX2319.

^d MIC with no compound/MIC with 25 μM PA β N.

^e MIC for WT/MIC for ΔacrB strain.

^f MIC for WT/MIC for ΔtolC strain.

and β -lactam antibiotics. Interestingly, the MIC shift produced by PA β N for rifampin was greater than that of the ΔacrB strain, suggesting an additional mechanism of action for PA β N.

MBX2319 does not perturb bacterial membranes. Because the AcrAB-TolC efflux pump utilizes the proton motive force (41), compounds that perturb the proton gradient across the cytoplasmic membrane can inhibit efflux through an indirect mechanism. To determine whether MBX2319 perturbs the transmembrane proton gradient, we measured uptake and accumulation of [³H]TMG in the presence of MBX2319 by the LacY permease, which

TABLE 4 TMG accumulation in *E. coli* NCM3722 in the presence of MBX2319

Compound	Concentration (μM)	TMG accumulation (mean \pm SD) (nmol/mg dry wt) ($n = 3$)	% control
None	0	4.4 \pm 0.4	100
None (–IPTG) ^a	0	0.1 \pm 0.0	3
CCCP	100	0.2 \pm 0.0	5
MBX2319	0.2	4.4 \pm 0.4	100
MBX2319	2	4.5 \pm 0.1	103
MBX2319	20 ^b	4.3 \pm 0.2	96

^a TMG accumulation in cells grown in the absence of IPTG.

^b The compound was slightly above the solubility limit in the assay buffer.

requires a proton motive force (42). The results are shown in Table 4. MBX2319 did not significantly inhibit uptake and accumulation of [³H]TMG at concentrations up to ~ 20 μM and thus does not inhibit efflux indirectly by perturbing the proton gradient.

PA β N has been shown to affect the integrity of the outer membrane, which is predicted to increase the rate of permeation of antibiotics into the periplasm (14). To determine whether MBX2319 affects the permeability of the outer membrane, we measured the influx of nitrocefin in a strain deficient in AcrAB (HN1159). The data shown in Table S3 in the supplemental material demonstrate that 20 μM MBX2319 does not increase the rate of nitrocefin influx, indicating no effect on outer membrane permeability.

Spectrum of activity. To determine whether MBX2319 inhibits the AcrAB-TolC orthologs of other Gram-negative pathogens, we measured the antibacterial activity of MBX2319 in combination with several antibiotics using three assays. First, we measured the MICs of several antibiotics, alone or in combination with MBX2319 or PA β N at a concentration of 25 μM , against several Gram-negative pathogens. The data are shown in Table 5. MBX2319 increased significantly the activity of CIP and LVX against the majority of the organisms tested, whereas PA β N (25 μM) did not significantly affect the MICs. MBX2319 and PA β N increased the activity of PIP and cefotaxime against the majority of organisms tested; however, MBX2319 was active against more organisms than was PA β N.

TABLE 5 Spectrum of activity of MBX2319

Organism	Drug ^a	MIC ($\mu\text{g/ml}$) for ^b :			MIC ratio for:	
		No EPI	MBX2319	PA β N	MBX2319 ^c	PA β N ^d
<i>Escherichia coli</i> AB1157	CIP	0.016	0.008	0.031	2	0.5
	LVX	0.031	0.016	0.031	2	1
	PIP	4	0.707	4	5.7	1
	CTX	0.1	0.022	0.25	4.8	0.42
<i>Escherichia coli</i> ATCC 25922	CIP	0.016	0.005	0.022	2.8	0.7
	LVX	0.031	0.013	0.022	2.4	1.4
	PIP	2.83	1.68	4	1.7	0.7
	CTX	0.074	0.063	0.25	1.2	0.3
<i>Escherichia coli</i> 331	CIP	128	32	128	4	1
	LVX	64	11.3	32	5.6	2
	PIP	4	0.707	4	5.6	1
	CTX	0.125	0.031	0.353	4	0.353
<i>Salmonella enterica</i> ATCC 14028	CIP	0.031	0.008	0.044	4	0.7
	LVX	0.062	0.016	0.044	4	1.4
	PIP	2.4	0.5	4	4.8	0.6
	CTX	0.21	0.063	0.297	3.4	0.7
<i>Shigella flexneri</i> ATCC 12022	CIP	0.031	0.008	0.031	4	1
	LVX	0.063	0.016	0.031	4	2
	PIP	1	0.25	1	4	1
	CTX	0.063	0.031	0.063	2	1
<i>Enterobacter aerogenes</i> ATCC 13048	CIP	0.037	0.008	0.031	4.8	1.2
	LVX	0.177	0.044	0.063	4	2.8
	PIP	4	1.4	16	2.8	0.2
	CTX	2	2.4	6.7	0.8	0.3
<i>Klebsiella pneumoniae</i> ATCC 700603	CIP	0.29	0.088	0.25	3.4	1.2
	LVX	0.71	0.149	0.5	4.7	1.4
	PIP	113	113	113	1	1
	CTX	8	8	8	1	1
<i>P. aeruginosa</i> PAO1	CIP	0.22	0.28	0.14	0.8	1.6
	LVX	1.6	2	0.89	0.8	1.8
	PIP	4	2	4	2	1
	CTX	8	4	8	2	1
<i>P. aeruginosa</i> ATCC 27853	CIP	0.21	0.125	0.149	1.7	1.4
	LVX	1	1	0.5	1	2
	PIP	16	19	19	0.84	0.8
	CTX	53.8	8	19	6.7	2.8

^a CIP, ciprofloxacin; LVX, levofloxacin; PIP, piperacillin; CTX, cefotaxime.

^b Geometric means of MICs from at least three replicate experiments are presented. The final concentration of the EPIs MBX2319 and PA β N was 25 μM .

^c MIC with no compound/MIC with 25 μM MBX2319.

^d MIC with no compound/MIC with 25 μM PA β N.

In addition, MBX2319 increased the activity of CIP and LVX against *E. coli* 331, which is resistant to fluoroquinolones. MBX2319 was not effective against *Proteus mirabilis* or any of the antibiotics tested (data not shown).

Second, a time-kill assay was used to verify the potentiating activity of 25 μM MBX2319 against Gram-negative pathogens (Fig. 2D). The combination of MBX2319 and a minimally bactericidal concentration of CIP (0.5 \times or 1 \times the MIC) decreased the viability of *Shigella flexneri*, *Salmonella enterica*, *Enterobacter aerogenes*, and *Klebsiella pneumoniae* by 100- to 1,000-fold, in comparison with CIP alone. In contrast, 25 μM PA β N was not effective

against any of the strains tested in this assay. Third, the H33342 accumulation assay was used to verify that MBX2319 inhibits efflux in other Gram-negative pathogens. The results of this assay are shown in Fig. 5A to H. MBX2319 (25 μM) increased H33342 accumulation in the majority of organisms tested, including *Shigella flexneri*, *K. pneumoniae*, *S. enterica*, and *Enterobacter cloacae*, and showed weak activity against *E. coli* 331 (CIP resistant), *P. mirabilis*, and *P. aeruginosa*.

MBX2319 increases the antibacterial activity of levofloxacin and piperacillin against a diverse panel of *E. coli* strains. To determine whether MBX2319 increases the antibacterial activity

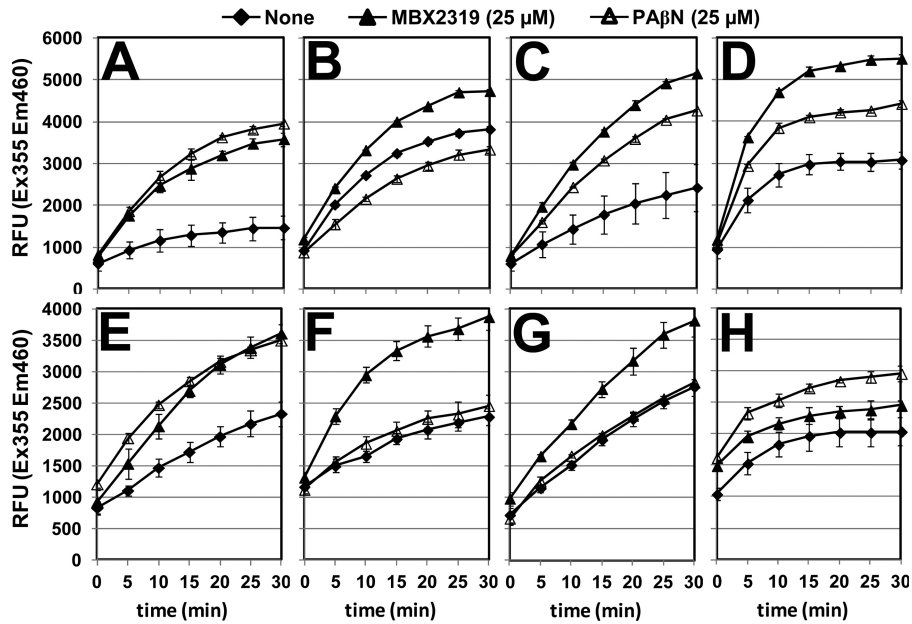


FIG 5 Effects of MBX2319 and PAβN on the accumulation of H33342 in various Gram-negative organisms. (A) *E. coli* AB1157. (B) *E. coli* 331. (C) *Shigella flexneri* ATCC 12022. (D) *Klebsiella pneumoniae* ATCC 13882. (E) *Salmonella enterica* (serovar Typhimurium) ATCC 14028. (F) *Enterobacter cloacae* subsp. *cloacae* ATCC 13047. (G) *Proteus mirabilis* ATCC 25933. (H) *Pseudomonas aeruginosa* ATCC 27835.

of LVX and PIP against a diverse panel of *E. coli* strains, we measured MICs for LVX and PIP in the absence and presence of 25 μM compound. The panel of 24 strains (see Table S4 in the supplemental material) is composed of strains that were publicly available clinical isolates; however, none of the strains was resistant to high levels of fluoroquinolones. Because the spectrum of activity includes the pathogens that are prevalent in urinary tract infections (UTIs), the *E. coli* panel included several strains isolated from UTIs. MBX2319 decreased the LVX MIC₅₀ and MIC₉₀ (the concentrations of LVX that inhibit growth of 50% and 90% of the strains, respectively) by 4-fold (Fig. 6). In contrast, MBX2319 did not have a significant effect on the PIP MIC₅₀ or MIC₉₀, probably because ~20% of the strains appeared to be resistant to PIP, as evidenced by the plateau in the cumulative percentage susceptible at ~80%, which is likely to be the result of β-lactamase expression.

Cytotoxicity. The cytotoxicity of MBX2319 against HeLa cells

was determined as described previously (37). The concentration of compound that reduced cell viability by 50%, the CC₅₀, was determined using a four-parameter curve-fitting algorithm (GraphPad Prism). The CC₅₀ for MBX2319 against HeLa cells was ≥100 μM; however, it is possible that the apparent lack of cytotoxicity is due, at least in part, to the relatively low aqueous solubility of this compound.

DISCUSSION

In this report, we describe the preliminary *in vitro* characterization of MBX2319, a novel inhibitor of the RND class AcrAB-TolC efflux pump, which is the major efflux pump in *E. coli* and other *Enterobacteriaceae* and plays a major role in the MDR phenotype of these pathogens (7). Our results demonstrate that MBX2319 exhibits the following characteristics of an EPI, as described by Lomovskaya et al. (14): (i) it potentiates the antibacterial activity

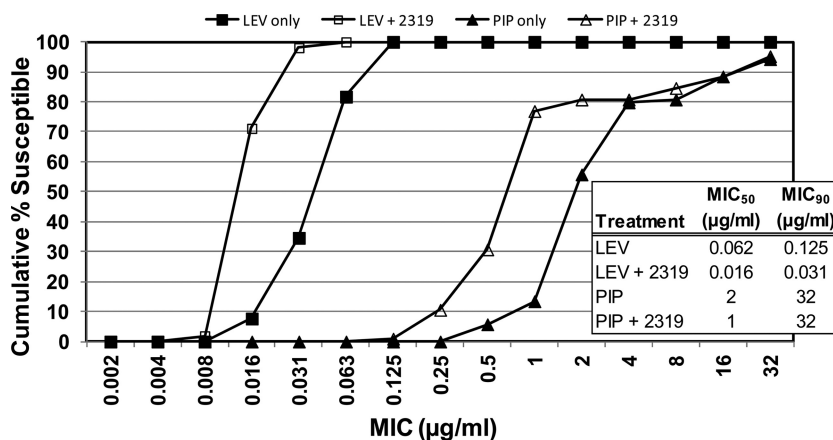


FIG 6 Cumulative MICs for levofloxacin (LEV) and piperacillin against a panel of 25 strains of *E. coli*, in the absence and presence of 25 μM MBX2319.

of diverse agents that are substrates of AcrAB-TolC, (ii) it does not potentiate the antibacterial activity of agents that are not substrates, (iii) it does not exhibit activity against mutants lacking functional AcrAB-TolC pumps, (iv) it inhibits the extrusion or accumulation of AcrAB-TolC substrates, and (v) it does not affect the energy source of AcrAB-TolC (proton gradient).

The most likely mechanism of inhibition of MBX2319 is through competitive inhibition and/or blockage of access to the substrate binding site of AcrB. However, our data do not rule out the possibility that MBX2319 inhibits other RND pumps, such as AcrF. The substrate binding pocket of AcrB is large, flexible, and rich in phenylalanine residues that define the binding pocket and interact with substrate molecules via hydrophobic and ring-stacking interactions (43, 44). Docking studies suggested that different pump substrates bind to distinct sites in the substrate binding pocket (45). However, it was unclear how inhibitors such as PA β N or 1-(1-naphthylmethyl)piperazine (NMP) could inhibit the extrusion of multiple chemically distinct substrates. The results of molecular dynamics simulations (46) suggested that PA β N and NMP interact with the “G-loop” (also known as the switch loop), which separates the access site and the substrate binding pocket. The G-loop is predicted to move substrates to the distal binding pocket through peristaltic action. Mutations that are predicted to prevent movement of the loop (G614P plus G621P and G616P plus G619P) abolished the efflux of doxorubicin and increased the sensitivity of the mutant strain to erythromycin (47). Therefore, efflux pump inhibitors could inhibit the efflux of diverse substrates by AcrB through binding to the G-loop. However, differences in the spectrum of compounds potentiated by MBX2319 versus PA β N suggest that MBX2319 binds to a different site in the AcrB binding pocket. Experiments that will further define the mechanism of MBX2319 are under way in our laboratories.

The pyranopyridine MBX2319 appears to be a novel EPI, as it is not structurally similar to any of the EPIs that have been described previously. However, a comparison of the structures of MBX2319 and other EPIs, such as the peptidomimetic PA β N and the pyridopyrimidine D13-9001 (12), reveals that these potent EPIs contain at least two hydrophobic ring systems, which presumably interact with hydrophobic residues in the substrate binding site. The activity exhibited by MBX2319 in *in vitro* assays was comparable or superior to that of PA β N at the same concentrations. Unlike PA β N, the activity of MBX2319 was not dependent on the presence of primary amines, which were required for activity and were responsible for the toxicity of PA β N and later analogs (24). The mechanism of action of MBX2319 appears to be through the exclusive inhibition of AcrAB-TolC, in contrast to PA β N, which also increases the permeability of the outer membrane (14). This additional mechanism was apparent in the potentiation of rifampin to levels greater than those of an Δ *acrB* strain (Table 3). Finally, MBX2319 possesses several drug-like properties, including a molecular weight of 409.54, a calculated logP value of 4.03, five hydrogen bond acceptors, zero hydrogen bond donors, a polar surface area of 45.49 Å², and two rotatable bonds. We are currently exploring the structure-activity relationship of this novel scaffold to develop analogs with improved activity.

MBX2319 is active against *E. coli* and other Gram-negative pathogens of the *Enterobacteriaceae* family, including *Shigella flexneri*, *K. pneumoniae*, *S. enterica*, and *E. cloacae*. In addition, MBX2319 significantly decreased the MICs for FQs against fluoroquinolone-resistant strains of *E. coli* (strains 331, 285, and 287),

but it did not overcome resistance caused by mutations in the FQ target. These results indicate a potential for broad-spectrum activity against pathogens of the *Enterobacteriaceae* family. The majority of published EPIs are not active against the MexAB-OprM efflux pump of *P. aeruginosa* (48), with the notable exceptions of PA β N (14) and DS-9001 (12), which exhibit activity against this pump. However, MBX2319 exhibited limited, but significant, activity against *P. aeruginosa*, suggesting that it may be possible to develop analogs with an extended spectrum of activity. AcrB and MexB are very similar in both primary structure (69.8% identity and 83.2% similarity) and three-dimensional structure (root mean standard deviation of 1.4 Å) (49). However, subtle differences in primary and tertiary structures appear to underlie the observed differences in substrate specificity (50). Because of the similarities that exist in the remainder of the substrate binding pocket, it may be possible to design analogs of MBX2319 with improved potency against MexB. Attempts to identify the potential sites of interaction of MBX2319 are under way.

Recent reports have underlined the importance of RND family efflux pumps in the MDR phenotype (7) and in resistance to fluoroquinolones and β -lactams in particular. MBX2319 potentiated the activity of fluoroquinolone and β -lactam antibiotics against *E. coli* and other important enterobacterial pathogens, such as *Shigella flexneri*, *Salmonella enterica* (serovar Typhimurium), *Enterobacter aerogenes*, *E. cloacae* (data not shown), and *Klebsiella pneumoniae*, that utilize RND family pumps. In addition, MBX2319 potentiated the activity of CIP and LVX against *P. aeruginosa* PAO1, a laboratory strain, but not against the reference strain ATCC 27854. However, the MIC of cefotaxime against ATCC 27854 was decreased significantly (~6-fold) by MBX2319. Taken together, the data suggest that MBX2319 has the potential to be active against important Gram-negative pathogens of the *Enterobacteriaceae* and *P. aeruginosa*. Based on the spectrum of activity versus Gram-negative pathogens and the classes of antibiotics that are potentiated by MBX2319, it could be useful as an adjunctive therapy in combination with a fluoroquinolone, β -lactam, or β -lactam/ β -lactamase inhibitor.

ACKNOWLEDGMENTS

This paper is dedicated to the memory of our late colleague Chad Housewartz.

The research reported in this article was supported by the National Institute of Allergy and Infectious Diseases of the National Institutes of Health (grants R43 AI074116 and R43 AI100332). G.C.W. is an American Cancer Society Professor and is supported by NIH grant R01 CA021615.

The content of this article is solely the responsibility of the authors and does not necessarily represent the official views of the National Institutes of Health.

REFERENCES

- Kang CI, Kim SH, Park WB, Lee KD, Kim HB, Kim EC, Oh MD, Choe KW. 2005. Risk factors for antimicrobial resistance and influence of resistance on mortality in patients with bloodstream infection caused by *Pseudomonas aeruginosa*. *Microb. Drug Resist.* 11:68–74. <http://dx.doi.org/10.1089/mdr.2005.11.68>.
- Kang CI, Kim SH, Park WB, Lee KD, Kim HB, Kim EC, Oh MD, Choe KW. 2005. Clinical epidemiology of ciprofloxacin resistance and its relationship to broad-spectrum cephalosporin resistance in bloodstream infections caused by *Enterobacter* species. *Infect. Control Hosp. Epidemiol.* 26:88–92. <http://dx.doi.org/10.1086/502492>.
- Kang CI, Kim SH, Park WB, Lee KD, Kim HB, Kim EC, Oh MD, Choe KW. 2005. Bloodstream infections caused by antibiotic-resistant Gram-negative bacilli: risk factors for mortality and impact of inappropriate

- initial antimicrobial therapy on outcome. *Antimicrob. Agents Chemother.* 49:760–766. <http://dx.doi.org/10.1128/AAC.49.2.760-766.2005>.
4. Kibbey CE, Poole SK, Robinson B, Jackson JD, Durham D. 2001. An integrated process for measuring the physicochemical properties of drug candidates in a preclinical discovery environment. *J. Pharm. Sci.* 90:1164–1175. <http://dx.doi.org/10.1002/jps.1070>.
 5. Peleg AY, Hooper DC. 2010. Hospital-acquired infections due to Gram-negative bacteria. *N. Engl. J. Med.* 362:1804–1813. <http://dx.doi.org/10.1056/NEJMra0904124>.
 6. Anthony KB, Fishman NO, Linkin DR, Gasink LB, Edelstein PH, Lautenbach E. 2008. Clinical and microbiological outcomes of serious infections with multidrug-resistant Gram-negative organisms treated with tigecycline. *Clin. Infect. Dis.* 46:567–570. <http://dx.doi.org/10.1086/526775>.
 7. Nikaido H, Pages JM. 2012. Broad-specificity efflux pumps and their role in multidrug resistance of Gram-negative bacteria. *FEMS Microbiol. Rev.* 36:340–363. <http://dx.doi.org/10.1111/j.1574-6976.2011.00290.x>.
 8. Nikaido H, Takatsuka Y. 2009. Mechanisms of RND multidrug efflux pumps. *Biochim. Biophys. Acta* 1794:769–781. <http://dx.doi.org/10.1016/j.bbapap.2008.10.004>.
 9. Piddock LJ. 2006. Clinically relevant chromosomally encoded multidrug resistance efflux pumps in bacteria. *Clin. Microbiol. Rev.* 19:382–402. <http://dx.doi.org/10.1128/CMR.19.2.382-402.2006>.
 10. Li XZ, Zhang L, Srikumar R, Poole K. 1998. Beta-lactamase inhibitors are substrates for the multidrug efflux pumps of *Pseudomonas aeruginosa*. *Antimicrob. Agents Chemother.* 42:399–403.
 11. Nakae T, Saito K, Nakajima A. 2000. Effect of sulbactam on anti-pseudomonal activity of beta-lactam antibiotics in cells producing various levels of the MexAB-OprM efflux pump and beta-lactamase. *Microbiol. Immunol.* 44:997–1001. <http://dx.doi.org/10.1111/j.1348-0421.2000.tb02595.x>.
 12. Yoshida K, Nakayama K, Ohtsuka M, Kuru N, Yokomizo Y, Sakamoto A, Takemura M, Hoshino K, Kanda H, Nitanai H, Namba K, Yoshida K, Imamura Y, Zhang JZ, Lee VJ, Watkins WJ. 2007. MexAB-OprM specific efflux pump inhibitors in *Pseudomonas aeruginosa*. Part 7: highly soluble and in vivo active quaternary ammonium analogue D13-9001, a potential preclinical candidate. *Bioorg. Med. Chem.* 15:7087–7097. <http://dx.doi.org/10.1016/j.bmc.2007.07.039>.
 13. Lomovskaya O, Lee A, Hoshino K, Ishida H, Mistry A, Warren MS, Boyer E, Chamberland S, Lee VJ. 1999. Use of a genetic approach to evaluate the consequences of inhibition of efflux pumps in *Pseudomonas aeruginosa*. *Antimicrob. Agents Chemother.* 43:1340–1346.
 14. Lomovskaya O, Warren MS, Lee A, Galazzo J, Fronko R, Lee M, Blais J, Cho D, Chamberland S, Renau T, Leger R, Hecker S, Watkins W, Hoshino K, Ishida H, Lee VJ. 2001. Identification and characterization of inhibitors of multidrug resistance efflux pumps in *Pseudomonas aeruginosa*: novel agents for combination therapy. *Antimicrob. Agents Chemother.* 45:105–116. <http://dx.doi.org/10.1128/AAC.45.1.105-116.2001>.
 15. Singh R, Swick MC, Ledesma KR, Yang Z, Hu M, Zechiedrich L, Tam VH. 2012. Temporal interplay between efflux pumps and target mutations in development of antibiotic resistance in *Escherichia coli*. *Antimicrob. Agents Chemother.* 56:1680–1685. <http://dx.doi.org/10.1128/AAC.05693-11>.
 16. Nishino K, Latifi T, Groisman EA. 2006. Virulence and drug resistance roles of multidrug efflux systems of *Salmonella enterica* serovar Typhimurium. *Mol. Microbiol.* 59:126–141. <http://dx.doi.org/10.1111/j.1365-2958.2005.04940.x>.
 17. Kvist M, Hancock V, Klemm P. 2008. Inactivation of efflux pumps abolishes bacterial biofilm formation. *Appl. Environ. Microbiol.* 74:7376–7382. <http://dx.doi.org/10.1128/AEM.01310-08>.
 18. Van Bambeke F, Pages JM, Lee VJ. 2006. Inhibitors of bacterial efflux pumps as adjuvants in antibiotic treatments and diagnostic tools for detection of resistance by efflux. *Recent Pat. Antiinfect. Drug Discov.* 1:157–175. <http://dx.doi.org/10.2174/15748910677452692>.
 19. Renau TE, Leger R, Filonova L, Flamme EM, Wang M, Yen R, Madsen D, Griffith D, Chamberland S, Dudley MN, Lee VJ, Lomovskaya O, Watkins WJ, Ohta T, Nakayama K, Ishida Y. 2003. Conformationally-restricted analogues of efflux pump inhibitors that potentiate the activity of levofloxacin in *Pseudomonas aeruginosa*. *Bioorg. Med. Chem. Lett.* 13:2755–2758. [http://dx.doi.org/10.1016/S0960-894X\(03\)00556-0](http://dx.doi.org/10.1016/S0960-894X(03)00556-0).
 20. Renau TE, Leger R, Flamme EM, Sangalang J, She MW, Yen R, Gannon CL, Griffith D, Chamberland S, Lomovskaya O, Hecker SJ, Lee VJ, Ohta T, Nakayama K. 1999. Inhibitors of efflux pumps in *Pseudomonas aeruginosa* potentiate the activity of the fluoroquinolone antibacterial levofloxacin. *J. Med. Chem.* 42:4928–4931. <http://dx.doi.org/10.1021/jm9904598>.
 21. Renau TE, Leger R, Flamme EM, She MW, Gannon CL, Mathias KM, Lomovskaya O, Chamberland S, Lee VJ, Ohta T, Nakayama K, Ishida Y. 2001. Addressing the stability of C-capped dipeptide efflux pump inhibitors that potentiate the activity of levofloxacin in *Pseudomonas aeruginosa*. *Bioorg. Med. Chem. Lett.* 11:663–667. [http://dx.doi.org/10.1016/S0960-894X\(01\)00033-6](http://dx.doi.org/10.1016/S0960-894X(01)00033-6).
 22. Renau TE, Leger R, Yen R, She MW, Flamme EM, Sangalang J, Gannon CL, Chamberland S, Lomovskaya O, Lee VJ. 2002. Peptidomimetics of efflux pump inhibitors potentiate the activity of levofloxacin in *Pseudomonas aeruginosa*. *Bioorg. Med. Chem. Lett.* 12:763–766. [http://dx.doi.org/10.1016/S0960-894X\(02\)00006-9](http://dx.doi.org/10.1016/S0960-894X(02)00006-9).
 23. Watkins WJ, Landaverry Y, Leger R, Litman R, Renau TE, Williams N, Yen R, Zhang JZ, Chamberland S, Madsen D, Griffith D, Tembe V, Huie K, Dudley MN. 2003. The relationship between physicochemical properties, in vitro activity and pharmacokinetic profiles of analogues of diamine-containing efflux pump inhibitors. *Bioorg. Med. Chem. Lett.* 13:4241–4244. <http://dx.doi.org/10.1016/j.bmcl.2003.07.030>.
 24. Lomovskaya O, Bostian KA. 2006. Practical applications and feasibility of efflux pump inhibitors in the clinic: a vision for applied use. *Biochem. Pharmacol.* 71:910–918. <http://dx.doi.org/10.1016/j.bcp.2005.12.008>.
 25. Nakayama K, Ishida Y, Ohtsuka M, Kawato H, Yoshida K, Yokomizo Y, Hosono S, Ohta T, Hoshino K, Ishida H, Yoshida K, Renau TE, Leger R, Zhang JZ, Lee VJ, Watkins WJ. 2003. MexAB-OprM-specific efflux pump inhibitors in *Pseudomonas aeruginosa*. Part 1: discovery and early strategies for lead optimization. *Bioorg. Med. Chem. Lett.* 13:4201–4204. <http://dx.doi.org/10.1016/j.bmcl.2003.07.024>.
 26. Nakayama K, Ishida Y, Ohtsuka M, Kawato H, Yoshida K, Yokomizo Y, Ohta T, Hoshino K, Otani T, Kurosaka Y, Yoshida K, Ishida H, Lee VJ, Renau TE, Watkins WJ. 2003. MexAB-OprM specific efflux pump inhibitors in *Pseudomonas aeruginosa*. Part 2: achieving activity in vivo through the use of alternative scaffolds. *Bioorg. Med. Chem. Lett.* 13:4205–4208. <http://dx.doi.org/10.1016/j.bmcl.2003.07.027>.
 27. Nakayama K, Kawato H, Watanabe J, Ohtsuka M, Yoshida K, Yokomizo Y, Sakamoto A, Kuru N, Ohta T, Hoshino K, Yoshida K, Ishida H, Cho A, Palme MH, Zhang JZ, Lee VJ, Watkins WJ. 2004. MexAB-OprM specific efflux pump inhibitors in *Pseudomonas aeruginosa*. Part 3: optimization of potency in the pyridopyrimidine series through the application of a pharmacophore model. *Bioorg. Med. Chem. Lett.* 14:475–479. <http://dx.doi.org/10.1016/j.bmcl.2003.10.060>.
 28. Nakayama K, Kuru N, Ohtsuka M, Yokomizo Y, Sakamoto A, Kawato H, Yoshida K, Ohta T, Hoshino K, Akimoto K, Itoh J, Ishida H, Cho A, Palme MH, Zhang JZ, Lee VJ, Watkins WJ. 2004. MexAB-OprM specific efflux pump inhibitors in *Pseudomonas aeruginosa*. Part 4: addressing the problem of poor stability due to photoisomerization of an acrylic acid moiety. *Bioorg. Med. Chem. Lett.* 14:2493–2497. <http://dx.doi.org/10.1016/j.bmcl.2004.03.007>.
 29. Yoshida K, Nakayama K, Kuru N, Kobayashi S, Ohtsuka M, Takemura M, Hoshino K, Kanda H, Zhang JZ, Lee VJ, Watkins WJ. 2006. MexAB-OprM specific efflux pump inhibitors in *Pseudomonas aeruginosa*. Part 5: carbon-substituted analogues at the C-2 position. *Bioorg. Med. Chem.* 14:1993–2004. <http://dx.doi.org/10.1016/j.bmc.2005.10.043>.
 30. Yoshida K, Nakayama K, Yokomizo Y, Ohtsuka M, Takemura M, Hoshino K, Kanda H, Namba K, Nitanai H, Zhang JZ, Lee VJ, Watkins WJ. 2006. MexAB-OprM specific efflux pump inhibitors in *Pseudomonas aeruginosa*. Part 6: exploration of aromatic substituents. *Bioorg. Med. Chem.* 14:8506–8518. <http://dx.doi.org/10.1016/j.bmc.2006.08.037>.
 31. Baba T, Ara T, Hasegawa M, Takai Y, Okumura Y, Baba M, Datsenko KA, Tomita M, Wanner BL, Mori H. 2006. Construction of *Escherichia coli* K-12 in-frame, single-gene knockout mutants: the Keio collection. *Mol. Syst. Biol.* 2:2006.0008. <http://dx.doi.org/10.1038/msb4100050>.
 32. Clinical and Laboratory Standards Institute. 2006. Method for dilution antimicrobial susceptibility testing for bacteria that grow aerobically; approved standard M7-A7. Clinical and Laboratory Standards Institute, Wayne, PA.
 33. Pillai SK, Moellering RC, Eliopoulos GM. 2005. Antimicrobial combinations, p 365–440. *In* Lorian V (ed), *Antibiotics in laboratory medicine*, 5th ed. Lippincott Williams & Wilkins, Philadelphia, PA.
 34. Coldham NG, Webber M, Woodward MJ, Piddock LJ. 2010. A 96-well plate fluorescence assay for assessment of cellular permeability and active efflux in *Salmonella enterica* serovar Typhimurium and *Escherichia coli*. *J.*

- Antimicrob. Chemother. 65:1655–1663. <http://dx.doi.org/10.1093/jac/dkq169>.
35. Nagano K, Nikaido H. 2009. Kinetic behavior of the major multidrug efflux pump AcrB of *Escherichia coli*. Proc. Natl. Acad. Sci. U. S. A. 106: 5854–5858. <http://dx.doi.org/10.1073/pnas.0901695106>.
 36. Bohnert JA, Karamian B, Nikaido H. 2010. Optimized Nile Red efflux assay of AcrAB-TolC multidrug efflux system shows competition between substrates. Antimicrob. Agents Chemother. 54:3770–3775. <http://dx.doi.org/10.1128/AAC.00620-10>.
 37. Butler MM, Lamarr WA, Foster KA, Barnes MH, Skow DJ, Lyden PT, Kustigian LM, Zhi C, Brown NC, Wright GE, Bowlin TL. 2007. Antibacterial activity and mechanism of action of a novel anilinouracil-fluoroquinolone hybrid compound. Antimicrob. Agents Chemother. 51: 119–127. <http://dx.doi.org/10.1128/AAC.01311-05>.
 38. Schumacher A, Steinke P, Bohnert JA, Akova M, Jonas D, Kern WV. 2006. Effect of 1-(1-naphthylmethyl)-piperazine, a novel putative efflux pump inhibitor, on antimicrobial drug susceptibility in clinical isolates of Enterobacteriaceae other than *Escherichia coli*. J. Antimicrob. Chemother. 57:344–348. <http://dx.doi.org/10.1093/jac/dki446>.
 39. Okusu H, Ma D, Nikaido H. 1996. AcrAB efflux pump plays a major role in the antibiotic resistance phenotype of *Escherichia coli* multiple-antibiotic-resistance (Mar) mutants. J. Bacteriol. 178:306–308.
 40. Ma D, Alberti M, Lynch C, Nikaido H, Hearst JE. 1996. The local repressor AcrR plays a modulating role in the regulation of *acrAB* genes of *Escherichia coli* by global stress signals. Mol. Microbiol. 19:101–112. <http://dx.doi.org/10.1046/j.1365-2958.1996.357881.x>.
 41. Zgurskaya HI, Nikaido H. 1999. Bypassing the periplasm: reconstitution of the AcrAB multidrug efflux pump of *Escherichia coli*. Proc. Natl. Acad. Sci. U. S. A. 96:7190–7195. <http://dx.doi.org/10.1073/pnas.96.13.7190>.
 42. Patel L, Garcia ML, Kaback HR. 1982. Direct measurement of lactose/proton symport in *Escherichia coli* membrane vesicles: further evidence for the involvement of histidine residue(s). Biochemistry 21:5805–5810. <http://dx.doi.org/10.1021/bi00266a013>.
 43. Eicher T, Cha HJ, Seeger MA, Brandstatter L, El-Delik J, Bohnert JA, Kern WV, Verrey F, Grutter MG, Diederichs K, Pos KM. 2012. Transport of drugs by the multidrug transporter AcrB involves an access and a deep binding pocket that are separated by a switch-loop. Proc. Natl. Acad. Sci. U. S. A. 109:5687–5692. <http://dx.doi.org/10.1073/pnas.1114944109>.
 44. Murakami S, Nakashima R, Yamashita E, Matsumoto T, Yamaguchi A. 2006. Crystal structures of a multidrug transporter reveal a functionally rotating mechanism. Nature 443:173–179. <http://dx.doi.org/10.1038/nature05076>.
 45. Takatsuka Y, Chen C, Nikaido H. 2010. Mechanism of recognition of compounds of diverse structures by the multidrug efflux pump AcrB of *Escherichia coli*. Proc. Natl. Acad. Sci. U. S. A. 107:6559–6565. <http://dx.doi.org/10.1073/pnas.1001460107>.
 46. Vargiu AV, Nikaido H. 2012. Multidrug binding properties of the AcrB efflux pump characterized by molecular dynamics simulations. Proc. Natl. Acad. Sci. U. S. A. 109:20637–20642. <http://dx.doi.org/10.1073/pnas.1218348109>.
 47. Nakashima R, Sakurai K, Yamasaki S, Nishino K, Yamaguchi A. 2011. Structures of the multidrug exporter AcrB reveal a proximal multisite drug-binding pocket. Nature 480:565–569. <http://dx.doi.org/10.1038/nature10641>.
 48. Pages JM, Amaral L. 2009. Mechanisms of drug efflux and strategies to combat them: challenging the efflux pump of Gram-negative bacteria. Biochim. Biophys. Acta 1794:826–833. <http://dx.doi.org/10.1016/j.bbapap.2008.12.011>.
 49. Sennhauser G, Bukowska MA, Briand C, Grutter MG. 2009. Crystal structure of the multidrug exporter MexB from *Pseudomonas aeruginosa*. J. Mol. Biol. 389:134–145. <http://dx.doi.org/10.1016/j.jmb.2009.04.001>.
 50. Tikhonova EB, Wang Q, Zgurskaya HI. 2002. Chimeric analysis of the multicomponent multidrug efflux transporters from Gram-negative bacteria. J. Bacteriol. 184:6499–6507. <http://dx.doi.org/10.1128/JB.184.23.6499-6507.2002>.
 51. Dewitt SK, Adelberg EA. 1962. The occurrence of a genetic transposition in a strain of *Escherichia coli*. Genetics 47:577–585.
 52. Soupene E, van Heeswijk WC, Plumbridge J, Stewart V, Bertenthal D, Lee H, Prasad G, Paliy O, Charernnoppakul P, Kustu S. 2003. Physiological studies of *Escherichia coli* strain MG1655: growth defects and apparent cross-regulation of gene expression. J. Bacteriol. 185:5611–5626. <http://dx.doi.org/10.1128/JB.185.18.5611-5626.2003>.
 53. Holloway BW. 1955. Genetic recombination in *Pseudomonas aeruginosa*. J. Gen. Microbiol. 13:572–581. <http://dx.doi.org/10.1099/00221287-13-3-572>.